ACS OMEGA

Open Access

http://pubs.acs.org/journal/acsodf

Article

White-Light Emission from a Host–Guest Composite between Carboxylatopillar[5]arene-Modified N-Doped Carbon Dots and Rhodamine 6G for Rutin Detection

Yun-qiong Yang,* Yuan Zhang, Yang Liu, Feier Lin, and Hao Zhang*

Cite This: *ACS Omega* 2024, 9, 14429–14435

Read Online

ACCESS | Metrics & More | Article Recommendations | Supporting Information

ABSTRACT: The construction of tunable white-light-emitting materials has garnered increasing attention in the scientific community. In this study, N-doped carbon dots (N-CDs) were surface-modified with carboxylatopillar[5]arene (CP[5]) using an EDC–NHS coupling reaction to create CCDs. CCDs were then conjugated with rhodamine 6G (R6G) through host–guest interactions to fabricate the CCDs–R6G composites. These composites produced two-color fluorescence emission peaks at 447 and 557 nm when excited by a wavelength of 340 nm. Excitingly, white-light emission (0.28, 0.30) can be readily achieved by varying the R6G concentration. To further explore potential applications, a new detection method for rutin (RT) based on the inner filter effect (IFE) was developed. Experimental results verify the practicality and reliability of the fluorescence sensor based on CCDs–R6G composites for RT detection in real samples.

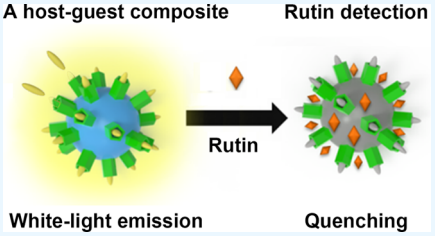

1. INTRODUCTION

Tunable multicolor luminescent materials have garnered significant attention due to their potential applications in biological imaging, light-emitting diodes, fluorescent sensors, photoelectric devices, and anticounterfeiting.[1−5] Among these materials, tunable white-light-emitting materials have attracted particular interest due to their advantages in visual observation. Conventional methods for obtaining such materials typically involve multiple components that emit different colors of light, including organic molecules, polymers, lanthanide-based metal–organic frameworks, semiconducting quantum dots, and more.[6−13] However, due to the environmental concerns associated with metals and the costly and laborious process of organic synthesis, it is crucial to develop inexpensive, environmentally friendly, and sustainable white-light-emitting materials.[14,15]

In contrast to conventional approaches, the supramolecular assembly approach based on macrocycles has emerged as a novel method for fabricating tunable white-light-emitting materials. This is because the host–guest interactions facilitated by macrocycles enable charge and energy transfer. Pillar[*n*]arene, a commonly used macrocyclic molecule, possesses stable structures, simple functionality, and superior host–guest properties. It finds applications in gas adsorption and separation, metal–organic frameworks, sensors, stimuli-responsive materials, biomedical applications, and more.[16−25] Additionally, the noncovalent nature of host–guest interactions imparts these materials with controllable, stimuli-responsive, and reversible properties.[26,27]

Carbon dots (CDs) have also made noteworthy advancements in fields such as biological imaging, catalysis, sensing, light-emitting diodes, and others.[28−33] Researchers have been captivated by their high stability, low toxicity, excellent emission properties, and ease of modification.[34−37] Rhodamine 6G (R6G), known for its exceptional optical properties such as high fluorescence quantum yield, large molar extinction coefficient, and emission wavelength in the long-wave region (>500 nm), is widely used in fluorescence applications.[38−40] Given that most CDs emit blue light when excited by UV light, R6G with its reddish-orange emission serves as an ideal cooperating emitter, as it complements the blue emission to produce white light.

In this study, we modified the surface of N-doped carbon dots (N-CDs) by coupling carboxylatopillar[5]arene (CP[5]) through an EDC–NHS reaction, resulting in the formation of CCDs. The CCDs–R6G composites were then created by attaching R6G onto the surface of CCDs via a host–guest interaction. This interaction effectively prevents the polymerization of dyes on the CCD surface and enhances the fluorescence emission. Under excitation at a wavelength of 340 nm, the CCDs–R6G composites exhibit two-color fluorescence emission peaks at 447 and 557 nm. Interestingly, by adjusting the concentration of R6G, we can achieve white-light emission with CIE 1931 coordinates of (0.28, 0.30), presenting a new strategy for dimming. Moreover, the excitation

Received: January 8, 2024
Revised: February 14, 2024
Accepted: February 22, 2024
Published: March 11, 2024

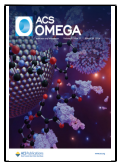

wavelength of the CCDs−R6G composites overlaps with the ultraviolet absorption peak of rutin. By utilizing the internal filtration effect (IFE), the dual-color fluorescence of the CCDs−R6G composites can be quenched, enabling the fluorescence detection of rutin (Scheme 1).

Scheme 1. Schematic Illustration of the Preparation Process of CCDs−R6G Composites and Their Application in the Field of Rutin Fluorescence Sensing

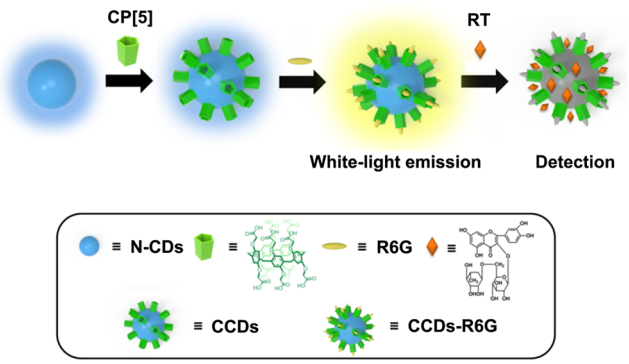

2. MATERIALS AND METHODS

2.1. General Information. Rhodamine 6G (R6G), citric acid, ethylenediamine, *N*-hydroxysuccinimide (NHS), and 1-ethyl-3-(3-(dimethylamino)propyl)carbodimide hydrochloride (EDC·HCl) were purchased from Aladdin. NaOH was obtained from Energy Chemical. Chlorine salts (Na^+, K^+, Ca^{2+}, Mg^{2+}), gallic acid, ascorbic acid, glucose, fructose, lysine, cysteine, and rutin were bought from Sinopharm Chemical Reagent Co., Ltd., China. Carboxylatopillar[5]arene (CP[5]) was synthesized according to our published procedure.[41]

Transmission electron microscopy (TEM) images were acquired by using a JEM 2100F instrument operating at an accelerating voltage of 200 kV. Fourier transform infrared (FTIR) spectra were obtained by using a Bruker Vertex 80 V spectrometer. Powder X-ray diffraction (PXRD) measurements were conducted by using a PANalytical B.V. Empyrean powder diffractometer. Ultraviolet−visible (UV−vis) spectra were recorded using a Shimadzu UV-2550 instrument. Thermogravimetric analysis (TGA) was performed on a Q500 instrument. Fluorescence spectra were recorded in quartz cuvettes by using a Shimadzu RF-5301PC spectrophotometer. ζ potentials were recorded on a Particle Sizing Systems Z3000 instrument.

2.2. Preparation of N-Doped Carbon Dots (N-CDs). N-doped carbon dots (N-CDs) were synthesized using the method described in a previous study.[42] In summary, a solution containing ethylenediamine (335 μL) and citric acid (1.051 g) dissolved in water (10 mL) was subjected to heating at 200 °C for a duration of 5 h. The reaction solution transitioned from colorless to brown, indicating the successful formation of N-CDs. Subsequently, N-CDs were obtained through the processes of dialysis and vacuum drying.

2.3. Preparation of CCDs. CP[5] (50 mg) was dispersed in deionized water (50 mL) and subjected to sonication for 5 min. Subsequently, EDC (300 mg) and NHS (540 mg) were added to the solution. After an additional sonication period of 20 min, N-CDs (50 mg) were introduced, and the resulting mixture was stirred at room temperature for 24 h. Following this, NaOH (50 mg) was added and stirred with the reaction mixture for 2 h. Upon completion of the reaction, the solution was dialyzed at room temperature for 3 days to eliminate the impurities.

2.4. Fluorescence Sensing Determination of Rutin. An 83.48 μM stock solution of R6G was prepared by using double-distilled water, while CCDs were dissolved in double-distilled water to create a 1.0 mg mL^{-1} aqueous solution. A

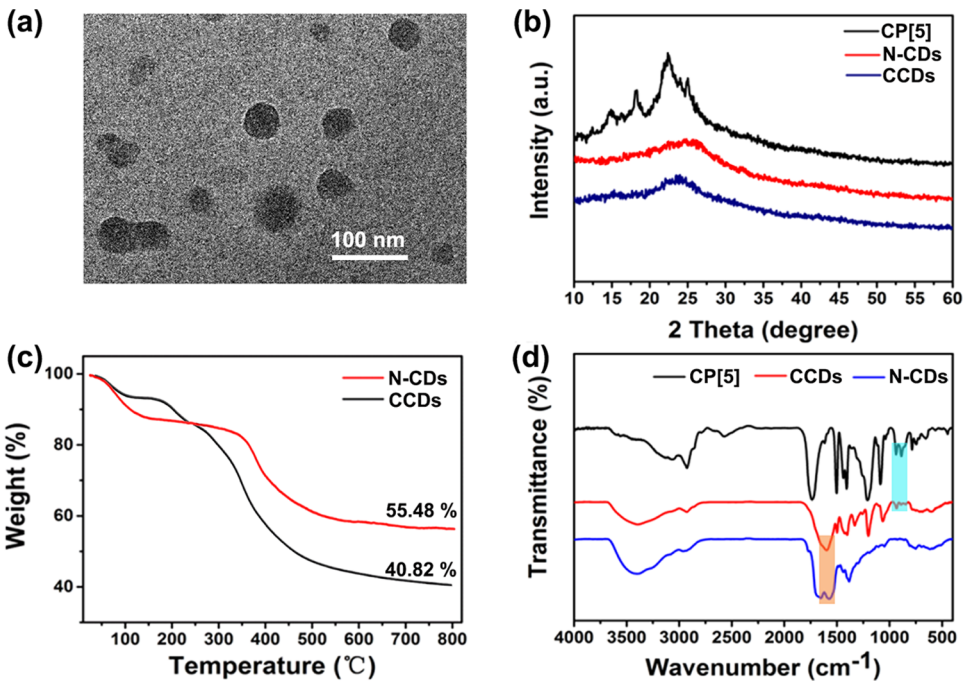

Figure 1. (a) TEM image of CCDs. (b) PXRD patterns of CP[5], N-CDs, and CCDs. (c) TGA curves of N-CDs and CCDs. (d) FTIR spectra of CP[5], N-CDs, and CCDs.

https://doi.org/10.1021/acsomega.4c00249
ACS Omega 2024, 9, 14429−14435

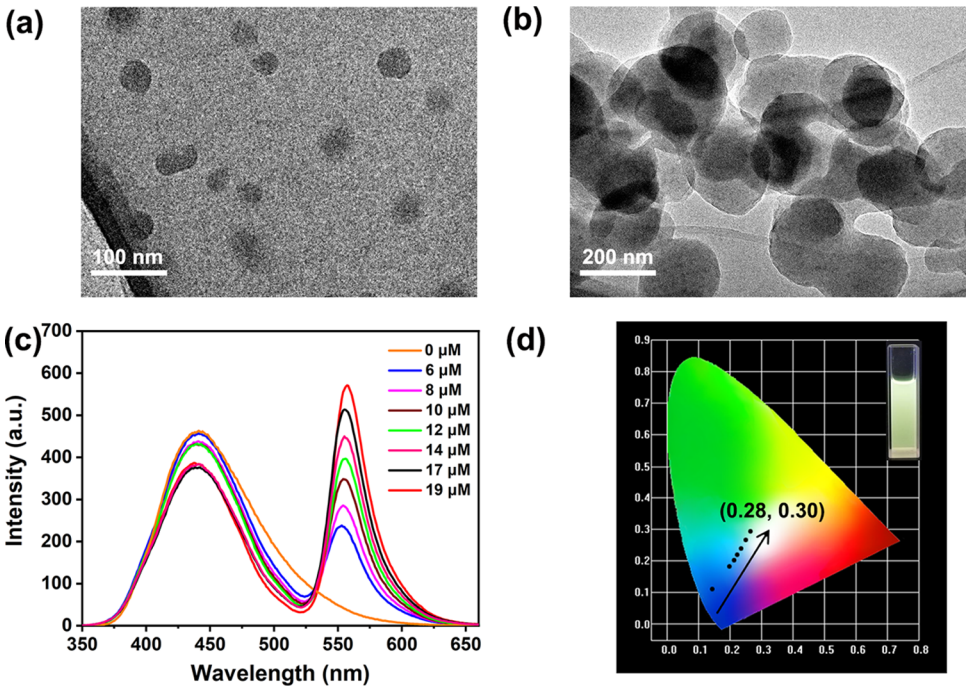

Figure 2. TEM images of (a) CCDs−R6G and (b) N-CDs−R6G. (c) Fluorescence emission spectra of CCDs−R6G composites in the presence of different concentrations of the R6G aqueous solution. The concentration of CCDs was 0.133 mg/mL. (d) CIE 1931 chromaticity diagram showing the emissions of fluorescence by changing the R6G concentration.

total of 265 μL of the CCD solution and 200 μL of the R6G solution were combined in a 2 mL cuvette. Subsequently, varying concentrations of rutin (RT) ethanol solution, ranging from 0 to 200 μM, were added to the cuvette, and the volume was adjusted with an aqueous solution to maintain a constant volume. All samples were prepared and measured at room temperature. Fluorescence measurements were conducted using excitation and emission slit widths of 3 and 3 nm, respectively, with an excitation wavelength of 340 nm.

2.5. Preparation of Real Samples. To assess the practicality of the suggested fluorescence sensing approach in practical samples, rutin tablets were supplemented with diverse rutin concentrations ranging from 0 to 20 μM. Subsequently, the CCDs−R6G and rutin samples with varying concentrations were combined and subjected to a 10-min incubation period at ambient temperature. Ultimately, the fluorescence emitted by rutin in the pharmaceutical samples was measured using the proposed CCDs−R6G probe. This entire process was repeated three times to ensure accuracy and consistency in the measurements.

3. RESULTS AND DISCUSSION

Transmission electron microscopy (TEM) was used to characterize the morphology of N-CDs, revealing the presence of small, spherical nanoparticles with a diameter of 30 nm (as depicted in Figure S1). Relatively, CCDs exhibited an average diameter of 40 nm (as shown in Figure 1a), indicating that the particle size changed significantly before and after the modification of CP[5]. The formation of the desired crystal structure was confirmed by analyzing the powder X-ray diffraction (PXRD) patterns of CCDs, as depicted in Figure 1b. The observed peaks exhibited a high degree of concordance with N-CDs and CP[5]. In addition, the UV−vis spectra of CCDs contained two characteristic peaks appearing at 293 and 342 nm (Figure S3a), which were consistent with the characteristic absorption peaks of N-CDs and CP[5], respectively. Due to a reduction in the number of free amino groups after an EDC−NHS coupling reaction, the fluorescence intensity of CCDs decreased compared to N-CDs (Figure S3b).

Table 1. CIE Coordinates of FL Emissions at Different R6G Concentrations for CCDs−R6G Composites

R6G concentration	CIE	
μM	X	Y
0	0.15	0.12
6	0.20	0.19
8	0.21	0.21
10	0.22	0.23
12	0.23	0.24
14	0.25	0.27
17	0.26	0.29
19	0.28	0.30

Moreover, the Fourier transform infrared (FTIR) spectra of N-CDs, CP[5], and CCDs were also obtained (Figure 1d). In the FTIR analysis, the ring vibrations at 937 cm^{-1} and the phenyl plane bending vibrations at 1500 cm^{-1} were observed on both CP[5] and CCDs.[43] The appearance of the same characteristic peaks reflected that CP[5] was successfully assembled on the surface of CCDs. Similarly, the distinctive N−H band (1575 cm^{-1}) was clearly detected in both CCDs and N-CDs, providing additional confirmation that the composition of CCDS encompasses CP[5] and N-CDs.[41] Furthermore, the utilization of thermogravimetric analysis (TGA, as shown in Figure 1c) allowed for the determination of the quantity of the CP[5] ring present on the surface of CCDs. The observed mass reduction at approximately 200 °C can be attributed to the thermal decomposition of the amino and oxygen functional groups situated on the surface of N-CDs,

https://doi.org/10.1021/acsomega.4c00249
ACS Omega 2024, 9, 14429−14435

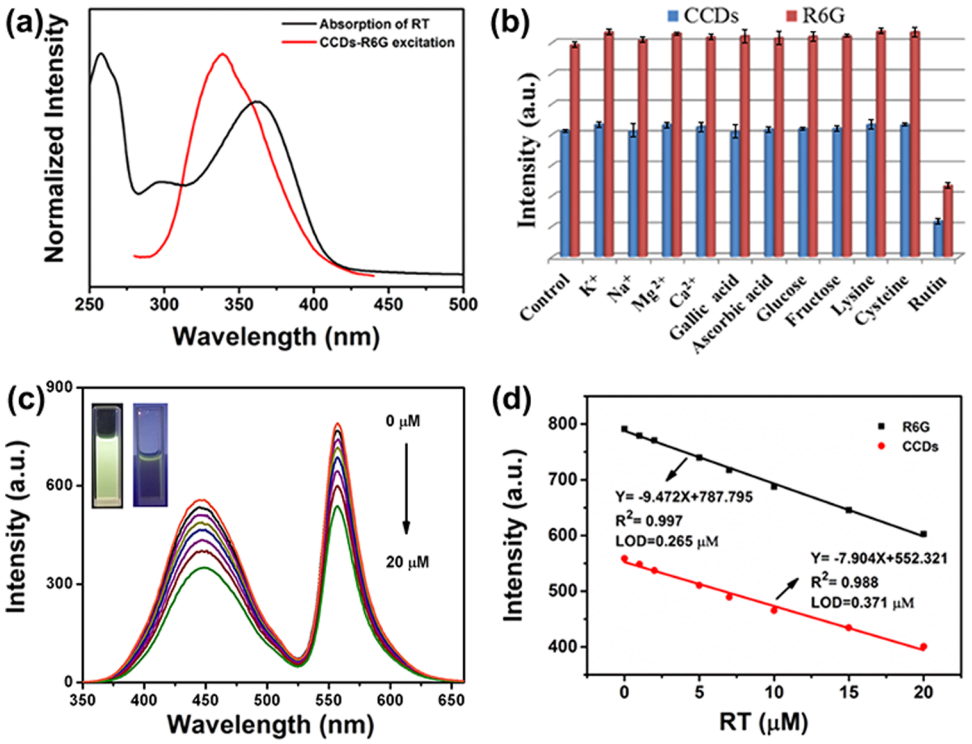

Figure 3. (a) UV−vis absorption spectra of RT (black line) and the excitation spectra of the CCDs−R6G composites (red line). (b) Fluorescence quenching degrees of the CCDs−R6G composites in the presence of various cations and other chemical compounds at the concentration of 100 μM. (c) Fluorescence spectra of rutin in ethanol solution upon addition of different amounts of rutin (0−20 μM). (d) FL emission spectra of composites with a good linear relationship at 447 and 557 nm versus different rutin concentrations.

Table 2. Analytical Results of RT in Real Samples from the Fluorescence Sensor[abc]

samples	added RT/μM	from CCDs/μM[c]	recovery/%	RSD/%[c]	from R6G/μM[c]	recovery/%	RSD/%[c]
1	0	not detected			not detected		
2	5	5.40 ± 0.16	107.64	3.19	4.78 ± 0.14	95.42	2.30
3	10	10.56 ± 0.21	106.45	3.10	9.76 ± 0.15	96.63	1.38
4	15	15.45 ± 0.30	103.70	2.04	15.05 ± 0.19	100.31	1.95
5	20	19.90 ± 0.42	99.62	3.32	19.10 ± 0.34	96.97	2.21

[a]Analytical results for the detection of rutin in tea samples (n = 3). [b]Results were expressed as the mean of three determinations ± standard deviation (SD). [c]Relative standard deviation (RSD) was defined as (SD/mean) × 100%.

resulting in a substantial mass loss of 44.52% up to 800 °C.[44] Additionally, the TGA analysis revealed that CCDs experienced a mass reduction at around 280 °C, which can be attributed to the pyrolysis of CP[5].[43] By subtracting the mass loss of N-CDs, it was estimated that the weight reduction caused by the pyrolysis of CP[5] in CCDs accounted for approximately 14.66%.

Under ultraviolet (UV) light excitation, the CCDs exhibited a pronounced blue fluorescence. This observation served as the impetus for the investigation of a fluorescent substance capable of emitting an orange hue, with the ultimate goal of establishing a luminescent system that produces white light. Following meticulous deliberation, the dye commonly known as rhodamine 6G (R6G) was selected due to its cost-effectiveness, elevated fluorescence quantum yield, and remarkable resistance to photodegradation. Additionally, R6G exhibited a strong affinity toward CP[5] on the CCDS surface via host−guest interaction, forming the CCDs−R6G composites.

The transmission electron microscopy measurements, as depicted in Figure 2a, indicated that the average particle size of the CCDs−R6G composite remained at 40 nm, exhibiting no substantial alteration. Under daylight conditions, the CCDs in water exhibited a faint yellow hue, while the CCDs−R6G mixture and pure R6G displayed distinct shades of pink (Figure S4). The UV−vis spectra of CCDs−R6G exhibited three distinct absorption peaks at 293, 348, and 531 nm, as depicted in Figure S5a. The findings indicate that the preparation of the CCDs−R6G composites was accomplished successfully. Furthermore, two prominent fluorescence emission peaks were observed, aligning with the characteristic emission peaks of both CCDs and R6G, as illustrated in Figure S5b. The emission amount at 447 nm exhibited a gradual decrease, while the emission intensity at 557 nm showed an increase with the increase in the R6G concentration (Figure 2c). The fluorescence colors of the CCDs−R6G composites demonstrated a linear transition from the blue to white region, as evidenced by the CIE 1931 chromaticity diagram (Figure 2d). Notably, the concentration of R6G at approximately 19 μM resulted in the observation of white-light emission at coordinates (0.28 and 0.30) (Table 1).

https://doi.org/10.1021/acsomega.4c00249
ACS Omega 2024, 9, 14429−14435

However, the control group, a mixture of N-CDs and R6G (known as N-CDs−R6G), did not exhibit white-light emission, as evidenced by Figure S6 and Table S1. The TEM measurements revealed an increase in the average particle size to approximately 200 nm for the N-CDs−R6G composites, as depicted in Figure 2b. Additionally, the ζ potential of the pristine N-CDs, initially measured at −22.08 mV, significantly decreased to −18.65 mV upon the introduction of R6G, as shown in Figure S7. This decrease can be attributed to the electrostatic interaction between the R6G molecules and negatively charged N-CDs. The variation in emission at 557 nm suggests that R6G molecules were adsorbed onto the surface of N-CDs, leading to a decrease in the emission intensity. These observations indicated that CCDs−R6G composites prepared by host−guest interactions have unique fluorescence properties.

CCDs−R6G composites introduced a novel approach for detecting rutin (RT). The absorption spectra of RT were observed to peak at 360 nm, which coincided well with the excitation spectra of the CCDs−R6G composites (Figure 3a). Consequently, the fluorescence intensity of the CCDs−R6G composites was effectively suppressed through the process of inner filter effect (IFE) in the presence of these two substances.[45−48] In order to assess the selectivity of CCDs−R6G composites, the potential interference from common cations (K^+, Na^+, Mg^{2+}, Ca^{2+}) and compounds (gallic acid, ascorbic acid, glucose, fructose, lysine, cysteine, and RT) was examined under identical experimental conditions. As depicted in Figure 3b, RT demonstrated an effective fluorescence intensity reduction in the CCDs−R6G composites. Conversely, the impact of other potential interfering substances on the fluorescence intensity of the CCDs−R6G composites is deemed insignificant.

The emission spectra of the CCDs−R6G composites were recorded at various concentrations of RT (0−20 μM), as depicted in Figure 3c. At a concentration of 20 μM, a significant decrease in the spectral peak was observed at 447 and 557 nm. Figure 3d demonstrates a strong linear correlation between the fluorescence intensity and the concentration of RT (0−20 μM) from CCDs and R6G, with coefficients of determination of 0.988 and 0.997, respectively. The limit of detection (LOD) for RT was determined to be 0.371 and 0.265 μM, using the signal-to-noise ratio method with a threshold of S/N = 3. These findings suggested that the CCDs−R6G composites served as a suitable probe for quantitative analysis.

To assess the analytical performance of the fluorescence sensor based on CCDs−R6G composites in rutin tablet samples, the obtained results using the standard addition method are presented in Table 2. Analysis of Table 2 revealed that the RT detection outcomes of the sensor for pharmaceutical samples, as determined by the linear plot at 447 nm from CCDs and 557 nm from R6G in Figure 3d, exhibited consistency with the predetermined RT concentration values. The average recovery of CCDs ranged from 99.56 to 107.74% (R6G exhibited a range of 95.4−100.3%), with corresponding RSD values of CCDs ranging from 2.03 to 3.31% (R6G exhibited a range of 1.38−2.31%). These findings provide further confirmation of the sensor's reliability and accuracy.

4. CONCLUSIONS

In conclusion, CP[5] was covalently modified with N-CDs via an EDC−NHS coupling reaction to produce CCD composites. Subsequently, CCDs−R6G composites were formed by immobilizing R6G onto the surface of CCDs through a host−guest interaction. The inclusion of CP[5] effectively mitigates dye aggregation on the CCD surface, resulting in white-light emission. To further advance the application of CCDs−R6G composites, a novel rutin (RT) detection method based on IFE was developed. This method exhibits robust resistance to interference, excellent stability, and high reliability. The CCDs−R6G composites were successfully employed in the analysis of real samples.

■ ASSOCIATED CONTENT

Supporting Information

The Supporting Information is available free of charge at https://pubs.acs.org/doi/10.1021/acsomega.4c00249.

TEM image of N-CDs; UV−vis spectra and fluorescence spectra of N-CDs, CP[5], CCDs, R6G, and CCDs−R6G; ζ potential diagram of N-CDs and N-CDs−R6G; and fluorescence decay curves of CCDs−R6G and CCDs−R6G−RT (PDF)

■ AUTHOR INFORMATION

Corresponding Authors

Yun-qiong Yang − *School of Environmental and Chemical Engineering, Jiangsu Ocean University, Lianyungang 222005, P. R. China*; Email: yz9502@163.com

Hao Zhang − *School of Environmental and Chemical Engineering, Jiangsu Ocean University, Lianyungang 222005, P. R. China*; orcid.org/0000-0002-4465-0991; Email: zhhao310@foxmail.com

Authors

Yuan Zhang − *School of Environmental and Chemical Engineering, Jiangsu Ocean University, Lianyungang 222005, P. R. China*

Yang Liu − *School of Environmental and Chemical Engineering, Jiangsu Ocean University, Lianyungang 222005, P. R. China*

Feier Lin − *School of Environmental and Chemical Engineering, Jiangsu Ocean University, Lianyungang 222005, P. R. China*

Complete contact information is available at: https://pubs.acs.org/10.1021/acsomega.4c00249

Notes

The authors declare no competing financial interest.

■ ACKNOWLEDGMENTS

This work was financially supported by Open-end Funds of Jiangsu Key Laboratory of Function Control Technology for Advanced Materials, Jiangsu Ocean University (No. jsklfctam 202208) and the Training Programs of Innovation and Entrepreneurship for College Students in Jiangsu Ocean University.

■ REFERENCES

(1) He, X. W.; Zhao, Z.; Xiong, L. H.; Gao, P. F.; Peng, C.; Li, R. S.; Xiong, Y.; Li, Z.; Sung, H. H. Y.; Williams, I. D.; Kwok, R. T. K.; Lam, J. W. Y.; Huang, C. Z.; Ma, N.; Tang, B. Z. Redox-Active AIEgen-

Derived Plasmonic and Fluorescent Core@Shell Nanoparticles for Multimodality Bioimaging. *J. Am. Chem. Soc.* **2018**, *140*, 6904−6911.
(2) Chen, D.; Bao, C.; Zhang, L.; Zhang, Q.; Wu, Z.; Li, Z. Y.; Sun, X. Q.; Wang, L.; Xiao, T. Dynamic Time-Dependent Emission in Solution and Stable Dual Emission in Solid Matrix Exhibited by a Single-Component Fluorescence System. *Adv. Funct. Mater.* **2024**, No. 2314093, DOI: 10.1002/adfm.202314093.
(3) Ren, D. X.; Tang, L.; Wu, Z. Y.; Zhang, Q. A.; Xiao, T. X.; Elmes, R. B. P.; Wang, L. Y. An Amphiphilic Molecule with a Single Fluorophore Exhibits Multiple Stimuli-responsive Behavior. *Chin. Chem. Lett.* **2023**, *34*, No. 108617.
(4) Sun, Y. Q.; Lei, Y. L.; Liao, L. S.; Hu, W. P. Competition between Arene−Perfluoroarene and Charge-Transfer Interactions in Organic Light-Harvesting Systems. *Angew. Chem., Int. Ed.* **2017**, *56*, 10352−10356.
(5) Li, D.; Yang, X. G.; Yan, D. P. Cluster-Based Metal−Organic Frameworks: Modulated Singlet−Triplet Excited States and Temperature-Responsive Phosphorescent Switch. *ACS Appl. Mater. Interfaces* **2018**, *10*, 34377−34384.
(6) Tu, D. S.; Leong, P.; Guo, S.; Yan, H.; Lu, C. S.; Zhao, Q. Highly Emissive Organic Single-Molecule White Emitters by Engineering o-Carborane-Based Luminophores. *Angew. Chem., Int. Ed.* **2017**, *56*, 11370−11374.
(7) Sarkar, S. K.; Kumar, G. R.; Thilagar, P. White Light Emissive Molecular Siblings. *Chem. Commun.* **2016**, *52*, 4175−4178.
(8) Ravindran, E.; Varathan, E.; Subramanian, V.; Somanathan, N. Self-assembly of A White-light Emitting Polymer with Aggregation Induced Emission Enhancement Using Simplified Derivatives of Tetraphenylethylene. *J. Mater. Chem. C* **2016**, *4*, 8027−8040.
(9) Shinde, S.; Asha, S. Temperature Sensitive Emission Color Tuning and White Light Emission in Segmented OPV Polymer: Perylene Bisimide Supramolecular Complex. *Macromolecules* **2016**, *49*, 8134−8145.
(10) Xiao, T. X.; Ren, D. X.; Tang, L.; Wu, Z. Y.; Wang, Q.; Li, Z. Y.; Sun, X. Q. A Temperature-responsive Artificial Light-harvesting System in Water with Tunable White-light Emission. *J. Mater. Chem. A* **2023**, *11*, 18419−18425.
(11) Diao, K.; Whitaker, D. J.; Huang, Z. H.; Qian, H. W.; Ren, D. X.; Zhang, L. L.; Li, Z. Y.; Sun, X. Q.; Xiao, T. X.; Wang, L. Y. An Ultralow-acceptor-content Supramolecular Light-harvesting System for White-light Emission. *Chem. Commun.* **2022**, *58*, 2343−2346.
(12) Roy, S.; Pramanik, S.; Bhandari, S.; Chattopadhyay, A. Surface Complexed ZnO Quantum Dot for White Light Emission with Controllable Chromaticity and Color Temperature. *Langmuir* **2017**, *33*, 14627−14633.
(13) Pramanik, S.; Bhandari, S.; Chattopadhyay, A. Zinc Quinolate Complex Decorated $CuInS_2$/ZnS Core/Shell Quantum Dots for White Light Emission. *J. Mater. Chem. C* **2017**, *5*, 7291−7296.
(14) Lou, X. Y.; Yang, Y. W. Manipulating Aggregation-Induced Emission with Supramolecular Macrocycles. *Adv. Opt. Mater.* **2018**, *6*, No. 1800668.
(15) Lou, X. Y.; Song, N.; Yang, Y. W. Enhanced Solution and Solid-State Emission and Tunable White-Light Emission Harvested by Supramolecular Approaches. *Chem.—Eur. J.* **2019**, *25*, 11975−11982, DOI: 10.1002/chem.201902700.
(16) Jie, K. C.; Zhou, Y. J.; Yao, Y.; Shi, B. B.; Huang, F. H. CO_2-Responsive Pillar[5]arene-Based Molecular Recognition in Water: Establishment and Application in Gas-Controlled Self-Assembly and Release. *J. Am. Chem. Soc.* **2015**, *137*, 10472−10475.
(17) Tan, L. L.; Zhu, Y. L.; Long, H.; Jin, Y. H.; Zhang, W.; Yang, Y. W. Pillar[n]arene-based Supramolecular Organic Frameworks with High Hydrocarbon Storage and Selectivity. *Chem. Commun.* **2017**, *53*, 6409.
(18) Tan, L. L.; Li, H. W.; Qiu, Y. C.; Chen, D. X.; Wang, X.; Pan, R. Y.; Wang, Y.; Zhang, S. X. A.; Wang, B.; Yang, Y. W. Stimuli-responsive Metal-organic Frameworks Gated by Pillar[5]arene Supramolecular Switches. *Chem. Sci.* **2015**, *6*, 1640−1644.
(19) Strutt, N. L.; Zhang, H.; Stoddart, J. F. Enantiopure Pillar[5]arene Active Domains within A Homochiral Metal−organic Framework. *Chem. Commun.* **2014**, *50*, 7455−7458.
(20) Li, X. S.; Li, Y. F.; Wu, J. R.; Lou, X. Y.; Han, J. Y.; Qin, J. C.; Yang, Y. W. A Color-tunable Fluorescent Pillararene Coordination Polymer for Efficient Pollutant Detection. *J. Mater. Chem. A* **2020**, *8*, 3651−3657.
(21) Wang, X.; Liu, Z. J.; Hill, E. H.; Zheng, Y. B.; Guo, G. Q.; Wang, Y.; Weiss, P. S.; Yu, J. H.; Yang, Y. W. Organic-Inorganic Hybrid Pillarene-Based Nanomaterial for Label-Free Sensing and Catalysis. *Matter* **2019**, *1*, 848−861.
(22) Wu, M. X.; Yang, Y. W. Metal−Organic Framework (MOF)-Based Drug/Cargo Delivery and Cancer Therapy. *Adv. Mater.* **2017**, *29* (23), No. 1606134, DOI: 10.1002/adma.201606134.
(23) Chi, X.; Ji, X.; Xia, D.; Huang, F. H. A Dual-Responsive Supra-Amphiphilic Polypseudorotaxane Constructed from a Water-Soluble Pillar[7]arene and an Azobenzene-Containing Random Copolymer. *J. Am. Chem. Soc.* **2015**, *137*, 1440−1443.
(24) Yang, J.; Dai, D. H.; Lou, X. Y.; Ma, L. J.; Wang, B. L.; Yang, Y. W. Supramolecular Nanomaterials Based on Hollow Mesoporous Drug Carriers and Macrocycle-capped CuS Nanogates for Synergistic Chemo-photothermal Therapy. *Theranostics* **2020**, *10*, 615−629.
(25) Song, N.; Lou, X. Y.; Ma, L. J.; Gao, H.; Yang, Y. W. Supramolecular Nanotheranostics Based on Pillarenes. *Theranostics* **2019**, *9*, 3075−3093.
(26) Zhang, H.; Liang, F.; Yang, Y. W. Dual-Stimuli Responsive 2D Supramolecular Organic Framework for the Detection of Azoreductase Activity. *Chem.—Eur. J.* **2020**, *26* (1), 198−205, DOI: 10.1002/chem.201904443.
(27) Zhang, H.; Wang, X.; Huang, K. T.; Liang, F.; Yang, Y. W. Green Synthesis of Leaning Tower[6]arene-Mediated Gold Nanoparticles for Label-Free Detection. *Org. Lett.* **2021**, *23*, 4677−4682.
(28) Chen, B. B.; Liu, M. L.; Huang, C. Z. Carbon Dot-based Composites for Catalytic Applications. *Green Chem.* **2020**, *22*, 4034−4054.
(29) Dhenadhayalan, N.; Lin, K. C.; Saleh, T. A. Recent Advances in Functionalized Carbon Dots Toward the Design of Efficient Materials for Sensing and Catalysis Applications. *Small* **2020**, *16* (1), No. 1905767, DOI: 10.1002/smll.201905767.
(30) Hama Aziz, K. H.; Omer, K. M.; Hamarawf, R. F. Lowering the Detection Limit Towards Nanomolar Mercury Ion Detection via Surface Modification of N-doped Carbon Quantum Dots. *New J. Chem.* **2019**, *43*, 8677−8683.
(31) Cheng, W. B.; Xu, J.; Guo, Z. Z.; Yang, D. W.; Chen, X. F.; Yan, W.; Miao, P. Hydrothermal Synthesis of N,S co-doped Carbon Nanodots for Highly Selective Detection of Living Cancer Cells. *J. Mater. Chem. B* **2018**, *6*, 5775−5780.
(32) Li, X. X.; Wang, Z. F.; Liu, Y.; Zhang, W. G.; Zhu, C. F.; Meng, X. G. Bright Tricolor Ultrabroad-band Emission Carbon Dots for White Light-emitting Diodes with A 96.5 High Color Rendering Index. *J. Mater. Chem. C* **2020**, *8*, 1286−1291.
(33) Wang, Q.; Gao, Y. X.; Wang, B. Y.; Guo, Y. Y.; Ahmad, U.; Wang, Y. Q.; Wang, Y.; Lu, S. Y.; Li, H.; Zhou, G. F. N-Codoped Oil-soluble Fluorescent Carbon Dots for A High Color-rendering WLED. *J. Mater. Chem. C* **2020**, *8* (13), 4343−4349, DOI: 10.1039/D0TC00016G.
(34) Ding, L.; Huang, K. T.; Li, S. A.; Zhou, J.; He, H.; Peng, Z. Z.; Chatterjee, S.; Liang, F. One-Pot Hydrothermal Synthesis of Carbon Quantum Dots with Excellent Photoluminescent Properties and Catalytic Activity from Coke Powders. *J. Fluoresc.* **2020**, *30*, 151−156.
(35) Liu, M. L.; Chen, B. B.; Li, C. M.; Huang, C. Z. Carbon Dots: Synthesis, Formation Mechanism, Fluorescence Origin and Sensing Applications. *Green Chem.* **2019**, *21*, 449−471.
(36) Tuerhong, M.; Xu, Y.; Yin, X. B. Review on Carbon Dots and Their Applications. *Chin. J. Anal. Chem.* **2017**, *45*, 139−150.
(37) Wang, X. H.; Qu, K. G.; Xu, B. L.; Ren, J. S.; Qu, X. G. Microwave Assisted One-step Green Synthesis of Cell-permeable Multicolor Photoluminescent Carbon Dots without Surface Passivation Reagents. *J. Mater. Chem.* **2011**, *21*, 2445−2450.

https://doi.org/10.1021/acsomega.4c00249
ACS Omega 2024, 9, 14429−14435

(38) Wang, W.; Lin, P.; Ma, L. H.; Xu, K. X.; Lin, X. L. Separation and Determination of Flavonoids in Three Traditional Chinese Medicines by Capillary Electrophoresis with Amperometric Detection. *J. Sep. Sci.* **2016**, *39*, 1357−1362.
(39) Roy, A.; Mukherjee, R.; Dam, B.; Dam, S.; Roy, P. A Rhodamine-based Fluorescent Chemosensor for Al^{3+}: Is It Possible to Control the Metal Ion Selectivity of A Rhodamine-6G Based Chemosensor? *New J. Chem.* **2018**, *42*, 8415−8425.
(40) Kim, H. N.; Lee, M. H.; Kim, H. J.; Kim, J. S.; Yoon, J. A New Trend in Rhodamine-based Chemosensors: Application of Spirolactam Ring-opening to Sensing Ions. *Chem. Soc. Rev.* **2008**, *37*, 1465−1472.
(41) Zhang, H.; Wu, J. R.; Wang, X.; Li, X. S.; Wu, M. X.; Liang, F.; Yang, Y. W. One-pot solvothermal synthesis of Carboxylatopillar[5]-arene-modified Fe_3O_4 magnetic nanopartices for ultrafast separation of cationic dyes. *Dyes Pigm.* **2019**, *162*, 512−516.
(42) Zhu, S. J.; Meng, Q. N.; Wang, L.; Zhang, J. H.; Song, Y. B.; Jin, H.; Zhang, K.; Sun, H. C.; Wang, H. Y.; Yang, B. Highly Photoluminescent Carbon Dots for Multicolor Patterning, Sensors, and Bioimaging. *Angew. Chem., Int. Ed.* **2013**, *52*, 3953−3957.
(43) Zhou, T.; Yu, H.; Liu, M. Q.; Yang, Y. W. Carboxylatopillarene-Modified Reduced Graphene Oxides with High Water Dispersibility for Fluorescent Dye Sensing. *Chin. J. Chem.* **2015**, *33*, 125−130.
(44) Gao, J.; Wu, M. X.; Dai, D. H.; Cai, Z.; Wang, Y.; Fang, W. H.; Wang, Y.; Yang, Y. W. N-doped Carbon Dots Covalently Functionalized with Pillar[5]arenes for Fe^{3+} Sensing. *Beilstein J. Org. Chem.* **2019**, *15*, 1262−1267.
(45) Li, C.; Liu, W. J.; Sun, X. B.; Pan, W.; Yu, G. F.; Wang, J. P. Excitation Dependent Emission Combined with Different Quenching Manners Supports Carbon Dots to Achieve Multi-mode Sensing. *Sens. Actuators, B* **2018**, *263*, 1−9.
(46) Li, G. L.; Fu, H. L.; Chen, X. J.; Gong, P. W.; Chen, G.; Xia, L.; Wang, H.; You, J. M.; Wu, Y. N. Facile and Sensitive Fluorescence Sensing of Alkaline Phosphatase Activity with Photoluminescent Carbon Dots Based on Inner Filter Effect. *Anal. Chem.* **2016**, *88*, 2720−2726.
(47) Su, K.; Xiang, G. Q.; Jin, X. R.; Wang, X.; Jiang, X. M.; He, L. J.; Zhao, W. J.; Sun, Y. M.; Cui, C. Gram-scale Synthesis of Nitrogen-doped Carbon Dots from Locusts for Selective Determination of Sunset Yellow in Food Samples. *Luminescence* **2022**, *37*, 118−126.
(48) Fan, H. H.; Xiang, G. Q.; Wang, Y. L.; Zhang, H.; Ning, K. K.; Duan, J. Y.; He, L. J.; Jiang, X. M.; Zhao, W. J. Manganese-doped Carbon Quantum Dots-based Fluorescent Probe for Selective and Sensitive Sensing of 2,4,6-trinitrophenol via an Inner Filtering Effect. *Spectrochim. Acta, Part A* **2018**, *205*, 221−226.

https://doi.org/10.1021/acsomega.4c00249
ACS Omega 2024, 9, 14429−14435